Journal of Mines, Metals and Fuels, *73(5): 1429-1440; 2025. DOI: 10.18311/jmmf/2025/48046*

Print ISSN : 0022-2755

Journal of Mines, Metals and Fuels

Contents available at: *www.informaticsjournals.co.in/index.php/jmmf*

Split Injection Strategy for Waste Cooking Oil Biodiesel- Hydrogen Fueled Reactivity Controlled Combustion (RCCI) Process

Amin Firoz Bashir[1*] and Duradundi Sawant Badkar[2]

[1]Department of Technology (DoT), Shivaji University, Kolhapur – 416004, Maharashtra, India; firozamin@yahoo.co.uk
[2]Sindhudurg Shikshan Prasarak Mandal's College of Engineering, Kankavali, Shindhudurg - 416602, Maharashtra, India

Abstract

Compression ignition engines using an electronically controlled Engine Management System (ECM) are gaining attention for a high-speed Electronic Control Unit (ECU) controlled governor with a closed-loop fuel management system. This enables the sharp cutting of fuel required for torque-based or demand speed applications. The stringent emissions regulations and inflation in fuel prices present a major challenge for the engine research community. This work investigates the potential of a split injection strategy along with reactivity-controlled compression ignition combustion process to achieve ultra–low Hydro-Carbon (HC), Carbon Monoxide (CO), Nitrogen Oxides (NO_x) -smoke trade at full load operation. For this purpose, the main fuel used is Hydrogen (H_2), and the pilot fuel used is Waste Cooking Oil Biodiesel (WCOBD) 20% blend with diesel 80% (v/v) as WCOBD20%. Split injection strategies parameters used are energy share, Pilot Injection Angle (PIA), and Main Injection Angle (MIA). The engine operated knock-free with hydrogen (5–15 LPM) as the Rate of Pressure Rise (RPR) remained below 6 bar/°CA and no hunting was observed.

Major Findings: *The results demonstrate effective combustion regulation with improved combustion efficiency using hydrogen at a 4ms injection duration (10 LPM volume flow rate), corresponding to approximately a 32% energy share. While balancing the trade-off between NOx-smoke and HC-CO emissions, Further retarded injection timing increased performance by 25% with HC-CO emission reduction up to 20% with a penalty of NO_x emissions by 5% and smoke emissions by 6% raise.*

Keywords: *Combustion, Emissions, Energy Share, Hydrogen, Reactivity Control, Split Injection Strategy, Waste Cooking Oil Biodiesel*

1.0 Introduction

As the world economy grows, the requirement for crude oil is also increasing rapidly. Most of the researchers have a great interest in compression ignition engines due to their high compression ratio and increased fuel economy. The compression ignition engines suffer from high nitrogen oxide and particulate matter emissions. In recent years, premixed charge compression ignition has attracted the attention of researchers by achieving high thermal efficiency and low emissions. In premixed charge compression ignition combustion, reduction of particulate matter can be done by proper mixing of air and fuel before the combustion, and the reduction of nitric oxide is by high exhaust gas recirculation rate as well as lean fuel-air mixture. However, due to its high flammability and low volatility of diesel, there are still some more problems that need to be solved in case of premixed charge compression ignition engine, such as ignition

**Author for correspondence*

control, formation of homogeneous mixture, excessive wall impingement and so on. To reduce these problems, the new concept called Reactivity Controlled Compression Ignition (RCCI) combustion strategy has been developed recently. The reactivity-controlled compression ignition uses two fuels of different physical properties and separate injection. The low-boiling-point fuel and high-octane-number fuel are injected into the intake port, while the diesel fuel is injected into the combustion chamber, so that stratified combustion takes place[1]. The reactivity-controlled compression ignition is an auto-ignition combustion strategy which is operated by in-cylinder mixing of gasoline and diesel fuels[2]. This type of combustion strategy makes an evolution from the premixed charge compression ignition concept, as air and fuel are mixed before the combustion. However, in reactivity-controlled compression ignition, fuel reactivity varies across the cylinder[3]. To generate the reactivity inside the cylinder, the fuel, which has a high octane number, is injected from the intake port, as well as the fuel which is having high cetane number is directly injected into the cylinder. The fuel reactivity can be distributed into global reactivity and reactivity gradient. The global reactivity is determined by the types of fuels and the amount of fuel introduced into the cylinder. The reactivity gradient can be varied with the strategy of injection, such as early or late injection of high octane and high cetane fuels. Both percentages, along with the injection strategy of each fuel, have an impact on reactivity-controlled compression ignition combustion[4]. Recent simulated and experimental studies reveal that reactivity-controlled compression ignition combustion is an effective ignition control, maintaining high efficiency and low emissions. The reactivity-controlled compression ignition combustion is a more promising low-temperature combustion technique than homogeneous charge compression ignition[5]. Research on RCCI combustion utilising methanol/diesel through NSGA-II indicates that increased methanol proportions and optimised start of injection improve fuel efficiency and reduce emissions. The Exhaust Gas Recirculation (EGR) rate and beginning temperature are critical factors, since less EGR and elevated temperatures amplify ringing severity[6]. In reactivity controlled compression ignition combustion, by adjusting the ratio of high cetane fuel and high octane fuel, the ignition timing can be controlled[7]. Reitz's study of internal combustion engine development emphasizes the need for new methods to reduce emissions and increase efficiency. Combustion methods like Homogeneous Charge Compression Ignition (HCCI) and RCCI improve fuel economy and reduce emissions, addressing performance and environmental challenges[8] In case of natural gas RCCI combustion depends on natural gas composition and engine speed; greater Wobbe number gas improves efficiency but increases NOx; lower Waste Nitrogen (WN) gas produces more incomplete combustion at lower speeds[9]. In reactivity-controlled compression ignition combustion, nitric oxide emissions were decreased with the introduction of cotton oil methyl ester biodiesel. The hydrocarbon emissions decreased at lower percentages of cotton oil methyl ester and increased at higher percentages of cotton oil methyl ester. Smoke emissions were decreased at full load with 30% of cotton oil methyl ester. The brake thermal efficiency was increased with the addition of cotton oil methyl ester[10].

In the view of the fuel management system in reactivity controlled compression ignition engines, many renewable fuels can still be utilised. Further investigation should be conducted into oxygenated fuels in reactivity-controlled compression ignition combustion[11]. Because of higher thermal efficiency and lower cost of operation of the dual fuel diesel-natural gas reactivity controlled compression ignition engine compared with single fuel conventional diesel combustion mode, reactivity controlled compression ignition engines are useful for light-duty on-road applications[12]. At low and medium loads, reactivity-controlled compression ignition showed a lower heat release rate and indicated thermal efficiency as the n-butanol ratio was increased. An increase in n-butanol ratio helps reduce soot emissions and increase carbon monoxide and hydrocarbon emissions[13]. Hydrogen in Internal Combustion Engines (ICEs) might reduce pollutants and boost energy efficiency. Hydrogen improves combustion performance, especially when combined with standard fuels, according to research. However, infrastructure and NOx emissions remain obstacles to wider implementation. Review research highlights CI engine performance. Hydrogen fuel in dual fuel mode reduced Brake Thermal Efficiency (BTE) and Exhaust Gas Combustion Temperature (EGT) by 2–22 % and increased Brake Specific Fuel Consumption (BSFC), Polypropylene (PP) and Heat Release Rate (HRR) by 36%, 23%, and 30%. Emission studies indicated HC and CO increased 30%, whereas smoke and NOx fell 20–60%[14]. Thorough testing of Common Rail Direct Injection (CRDi) engines running hydrogen fuel and *Ceiba Pentandra* biodiesel reveals quite high efficiency and pollution reductions. Including hydrogen into combustion lowers

dangerous pollutants and increases thermal efficiency. NOx, HC and CO in the CRDi engine were decreased by 28%, 8.5% and 17%, respectively. EGR decreased BTE by about 14.2% and lowered HC, CO, and NOx by 6.3%,9% and 30.5%, respectively[15]. The performance of the CRDi engine using a combination of hydrogen and used Temple Oil Biodiesel (BTO). The analysis revealed that BTO and diesel both had a peak High Frequency Resistance (HFR) of 0.24 at 800 bar IP and bTDC IT. Dual Fuel (DF) CRDi engines featuring Toroidal Reentrant Combustion Chamber (TRCC) configurations exhibited a 6% reduction in BTE and a 19% increase in NOx emissions at full load conditions[16].

2.0 Experimental Facility and Processing Tools

2.1 RCCI Engine Details

A single-cylinder four-stroke direct-injected water-cooled diesel engine operated with a programmable open ECU is studied. The specifications of the engine used for the experiments are listed in the Table 1. The equipment and techniques used for emission measurement are summarized in Table 2. The sensors integrated into the engine test setup for various parameter measurements are listed in Table 3 the relationship between hydrogen flow rate and injector open time used in the RCCI experiments is provided in Table 4.

Table 1. Specifications of the engine[17,18]

Make and Model	Kirloskar, TV1
No. of Cylinders	One
Orientation	Vertical
Cycle	4 Stroke
Ignition System	Compression Ignition
Bore X Stroke	87.5mm X 110mm
Displacement Volume	660 cc
Compression Ration	18: 1
Arrangement of valves	Overhead
Combustion Chamber	Open Chamber (Direct Injection)
Rated Power	3.5 kW (5.2HP) @1500 rpm
Cooling Medium	Water cooled
RCCI Fuel- Low reactive fuel (LRF)	Hydrogen
Hydrogen Type	Hydrogen used is from a hydrogen tank stored at 150 bar and a delivery pressure of 2 bar. This was industrial-grade gray type hydrogen manufactured from non-renewable sources.
Pilot fuel injection (PFI) Injector Hydrogen	High impedance injector (3ms, 4ms, 5ms) Single Hole, 2 bar to 7 bar working pressure
RCCI Fuel High reactive fuel (HRF)	WCOBD 20% blend
Direct Injection (DI) injector	Peak n hold type low impedance IOP: 60MPa and MIA: 18, 23, 28 ^{0}bTDC and PIA: 28, 31, and 34 ^{0}bTDC

Table 2. Emission measurement details[17,18]

Sr. No.	Pollutant	Analyser Working Principle	Accuracy
1	Carbon Monoxide (CO)	NDIR (Non-Dispersive Infra-Red)	CO = +/- 0.2% CO
2	Carbon Dioxide (CO_2)	NDIR (Non-Dispersive Infra-Red)	CO_2 = +/- 1% CO_2
3	Nitrogen Oxide (NOx)	CLD (Chemiluminisent Detector)	NO_x = +/- 10 ppm NO
4	Hydrocarbons (HC)	FID (Flame Ionization Detector)	O_2 = +/- 0.2% O_2
5	Particulate Matter (PM)	PTFE (Poly Tetrafluoro Ethylene) Filter paper method	HC = +/- 30 ppm HC

Table 3. Sensors used for measurement[17]

Sr	Number	Description/Location	Unit	Sensor/Device
1	(T1)	Engine Jacket Water Inlet Temperature	°C	RTD PT 100
2	(T2)	Engine Jacket Water Outlet Temperature	°C	RTD PT 100
3	(T3)	Exhaust Calorimeter Water In Temperature	°C	RTD PT 100
4	(T4)	Exhaust Calorimeter Water Out Temperature	°C	RTD PT 100
5	(T5)	Exhaust Gas Temperature Before Calorimeter. (Engine)	°C	Thermocouple K type
6	(T6)	Exhaust Gas Temperature After Calorimeter. (Calorimeter)	°C	Thermocouple K type
7	(F7)	Air Flow Transmitter	mmWC	Pressure transmitter
8	(F8)	Fuel Flow Transmitter	mmWC	Differential Pressure Transmitter (DPT)
9	(F9)	Load Cell Sensor	kg	Strain Gauge
10	(P10)	Cylinder Pressure Transducer	bar	PCB pizoelectronics USA
11	(R12)	Engine Rpm (CA) Sensor	Crank Angle	Encoder
12	(F3)	Engine Jacket Cooling Water Flow Rate	LPH	Rotameter
13	(F4)	Calorimeter Cooling Water Flow Rate	LPH	Rotameter

Table 4. Hydrogen flow rate with injector open time[17,18]

Fuel Line Pressure	Injector Open Time From ECU	H_2 Mass Flow	H_2 Volume Flow	H_2 Volume Flow
Bar	Ms	kg/h	LPM	cc/min
2	0	0.0000	0.000	0
2	3	0.02	5.07	5070.14
2	4	0.05	10.13	10129.35
2	5	0.07	15.18	15184.89

2.2 Characteristics of Hydrogen Fuel Handling

This work uses gray hydrogen as the low-reactivity fuel. Made industrially from non-renewable sources, it is kept in 7 m^3 gas cylinders with a capacity allowing up to 0.5 kg of compressed hydrogen. With a supply pressure between 100 and 150 PSI, the storage conditions consist of a test pressure (TP) of 335–350 bar and a working pressure (WP) of 200 bar. Together with high-pressure gas pipelines rated at 25 MPa, hydrogen is handled safely utilizing flame arresters and wet flame arresters. To guarantee exact fuel metering, hydrogen gas is delivered into the intake. As shown in Table 5, a light absorption-based smoke meter was used to quantify smoke emissions at various engine loads. As illustrated in Figure 1, hydrogen was injected into the intake manifold while WCO biodiesel B:20 was directly injected into the cylinder as the high-reactivity fuel.

manifold in milliseconds (ms) via a solenoid injector.

Using hydrogen in this dual-fuel RCCI combustion system helps to greatly lower smoke emissions, CO and HC. As so, it presents possible advantages for society by encouraging better combustion and lowering environmental pollution.

3.0 Results and Discussion

3.1 Combustion Analysis

3.1.1 In-Cylinder Combustion Pressure Maximum

This is shown below in Figure 2, RCCI combustion with MIA 28^{0}bTDC and PIA 28^0 before Top Dead Center (bTDC)

Table 5. Smoke meter emissions device details[17,18]

AVL437 Standard	Smoke Opacity Measurement		Approval: ARAI Pune	
Measurement range	430 mm ±5 mm		Optical measurement principle	
Measurement	Range	Resolution	Suitable for full acceleration and full load testing	
Absorption (K Value)	0 to 99.99 m^{-1}	0.01 m^{-1}	Standard: ECE-24 and ISO 3173	
Opacity	0 to 100%	0.1 %	Customers: IIT, BMW, Maruti, Bajaj, Skoda, Automobile sector	
Engine speed (RPM)	400 to 6000 min^{-1}	1 min^{-1}	Compatible with HSU	
Oil temperature	0 to 150 ^{0}C	1 ^{0}C	As per M.O.R.T.H specifications	
Linearity check	≈ 50% of the measured range		RS232 interface	Auto Calibration

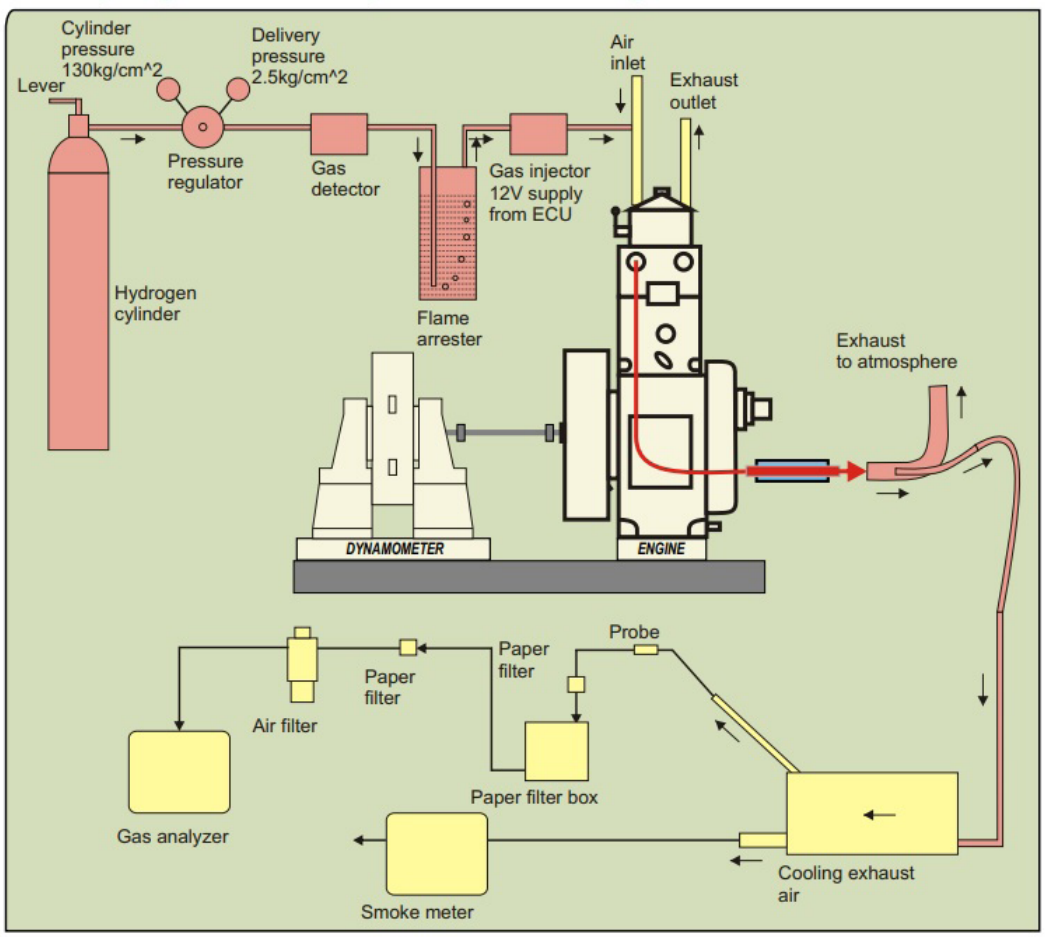


Figure 1. Experimental setup with Hydrogen RCCI.[16]

for all H_2 flow rates has shown more combustion pressure among other MIA-PIA operations. This may be due to sufficient compression pressure and temperature to form a homogeneous charge and simultaneous combustion. It is followed by MIA23^0 bTDC - PIA31^0 bTDC. However, PIA 34^0 bTDC has shown lower combustion pressure due to too advanced injection timings. In cylinder pressure, 50 bar reported by MIA-PIA 28^{0}bTDC 5ms is the highest among all other operations. Further, PIA34 showed a 20% lower in cylinder maximum pressure for all MIA and hydrogen fuel due to too advanced injection and may be an increased ignition delay.

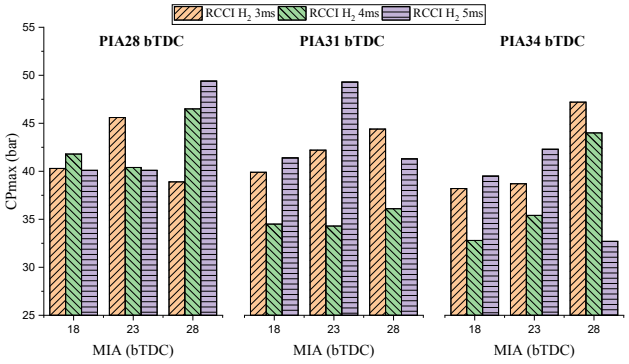


Figure 2. Cylinder pressure maximum for split injection WCOBD20-H_2 RCCI.

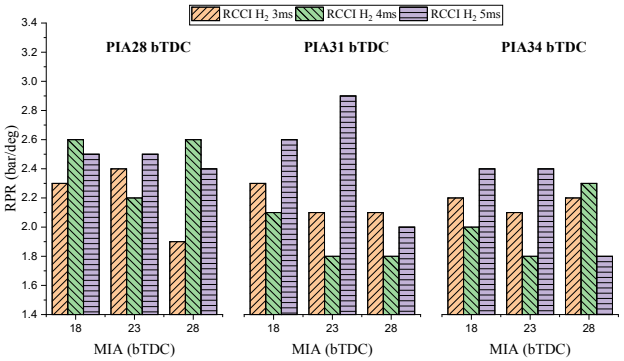


Figure 3. Rate of pressure rise (RPR) for split injection WCOBD20-H_2 RCCI.

3.1.2 Rate of Pressure Rise (RPR)

Figure 3 shows that decrease in RPR values with an increase in PIA angle. This shows that due to advanced timing, MIA28 and PIA34, lower in-cylinder combustion temperature and pressure are present. Also, a high H_2 flow rate with advanced timing absorbs more latent energy from compressed air to reach self-ignition temperature. In overall reduced combustion efficiency. Further MIA23^0 bTDC-PIA31^0 bTDC showed RPR up to 3 bar/deg CA. Also, H_2 flow rate with 5 ms showed higher RPR for all operations due to more flame speed of hydrogen increasing more rapid combustion.

3.1.3 Neat Heat Release Rate (NHRR)

It can be seen from neat heat release rate (NHR) graphs, Figure 4, that PIA31^0 and PIA34^0 at MIA28^0 showed too high NHR for the same power operation (3.5 kW) compared to other injection strategies. As low reactive fuel causes enriched hydrogen charge into the combustion

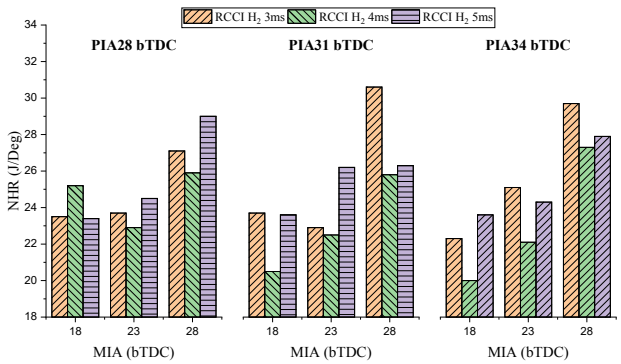


Figure 4. Neat heat release rate for split injection WCOBD20-H_2 RCCI.

chamber with an early injection of (PIA34^0 bTDC and PIA31^0 bTDC with MIA28^0 bTDC), high reactive fuel WCOBD20 causes rapid combustion, thus peak raises in HRR are observed. This produces knocking and reduces combustion efficiency similarly to retarded injection of MIA18^0 bTDC and PIA28^0 bTDC. On the other hand, controlled combustion and NHR are observed at MIA 28^0 bTDC and PIA28^0 bTDC as a consequence of not too low NHR or too high NHR.

3.1.4 Combustion Duration

Combination Duration is nothing but the End of Combustion (EOC) – the start of combustion (SOC) at deg crank angle. As the engine is constant speed of 1500 RPM, it is formulated that 9^0 crank angle is 1 millisecond (1ms) duration. Hence, as seen from the combustion duration shown in Figure 5 below varies from 7 ms to 9 ms or 65^0 crank angle (CA) to 90^0 CA. It can be seen that at early injection, PIA34^0 bTDC-MIA28^0 bTDC, more combustion duration (prolonged) is observed, leading to knocking and initial high NHRR. Also, peak combustion will be before TDC, causing a loss in torque and performance. On the other hand, PIA31^0 and MIA18^0, MIA23^0 showed short combustion duration. This leads to a sudden rise in RPR, NHR, and combustion pressure at TDC. This causes uncontrolled combustion. However, PIA28^0 with all RCCI hydrogen energy shared moderate combustion duration and showed a controlled combustion approach. This results in more combustion efficiency, and simultaneous combustion instead of instantaneous combustion in the other two (PIA34^0 bTDC and PIA31 ^{0} bTDC) injection strategies.

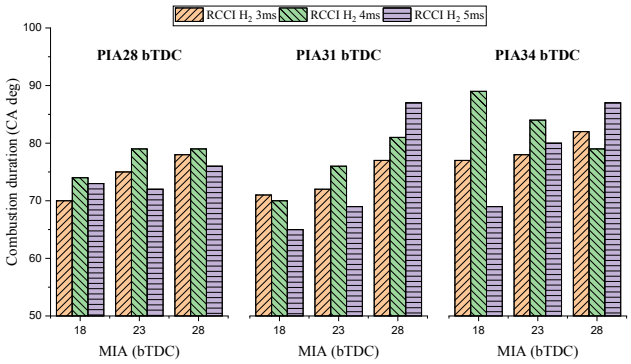


Figure 5. Combustion duration for split injection WCOBD20-H_2 RCCI.

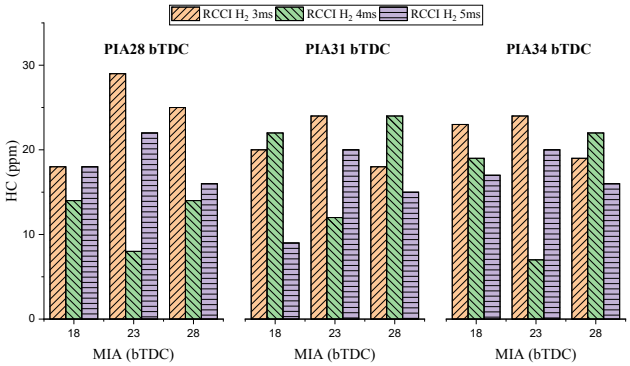


Figure 6. Hydrocarbon emissions for split injection WCOBD20-H_2 RCCI.

3.2 Emissions Analysis

3.2.1 Hydro-Carbon Emissions

As seen from Figure 6 below, less HC emissions are observed for H_2 flow rate (10.2 litres per min (LPM) and 15.9 LPM) with injector open time 4 ms and 5 ms, respectively, compared to 3ms (5.6 LPM) H_2 flow rate. Further, at MIA 23^0 bTDC and PIA 28^0 bTDC, HC emissions are reported to be the least compared to all other operations. PIA34^0 bTDC and PIA31^0 bTDC with all MIA and PIA28^0 bTDC with 18^0 bTDC and 23^0 bTDC MIA showed more HC emissions due to more stratified zones in combustion and lower combustion efficiency. It can be noted that the least HC emissions of 9 parts per million (ppm) with an H_2 flow rate of 10.2 LPM (4ms injector open time) at MIA23^0 bTDC –PIA28^0 bTDC fuel injection timing.

3.2.2 Carbon Monoxide Emissions (CO)

These are a result of incomplete combustion, shown in Figure 7. It can be seen that RCCI fuel with a 3ms injector open time of 5.6 LPM H_2 flow rate has shown more CO emissions for all injection timings. This may be due to less energy shared hydrogen fuel compared to 4 ms and 5 ms injector times. A lower energy share of hydrogen fuel means a higher energy share of carbon fuel, like highly reactive fuel (WCOBD20). Hence, CO emissions can be reduced with more hydrogen energy. Further, the least CO emissions are reported at MIA 23^0 bTDC timing and 4ms (10.2 LPM) hydrogen flow rate. Also, a higher hydrogen flow rate with advanced injection timing of PIA31^0 bTDC and PIA34^0 bTDC showed more stratified reach and lean zones, causing more instantaneous combustion. It can be

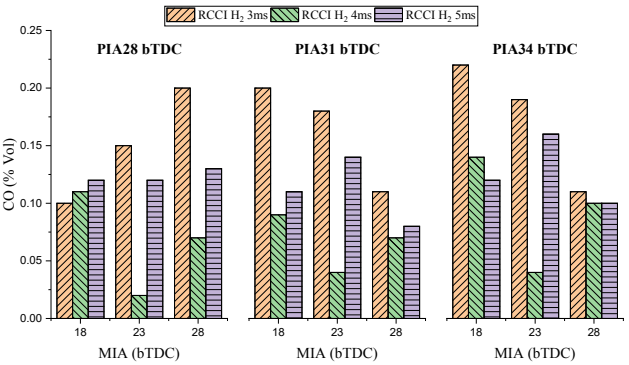


Figure 7. Carbon monoxide emissions for split injection WCOBD20-H_2 RCCI.

noted that PIA34^0 bTDC and PIA34^0 bTDC show more CO emissions than MIA23^0 bTDC injection timing and 4ms due to more stratified zones.

3.2.3 Nitric Oxides Emissions

Nitric Oxides Emissions with RCCI fuel combination and fuel injection strategy show Figure 8, reduced NOx emissions at MIA 23^0 bTDC-PIA 28^0 bTDC and 4ms (10.22 LPM) hydrogen fuel flow rate. This may be due to more controlled and reactivity control combustion with a strategic injection timing approach. This injection timing, MIA 23^0 bTDC-PIA 28^0 bTDC, and 4ms (10.22 LPM) hydrogen fuel flow is 50% less compared to the same injection timing and higher hydrogen or WCOBD energy share. This highlights optimized reactivity stratification with controlled High Reactive Fuel (HRF) and Low Reactive Fuel (LRF) energy share along with an advanced PIA 28^{0}bTDC injection timing strategy to reduce temperature heterogeneities and achieve

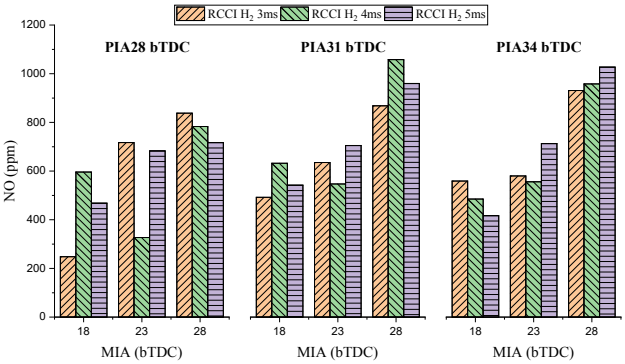


Figure 8. Nitric oxide emissions for split injection WCOBD20-H_2 RCCI.

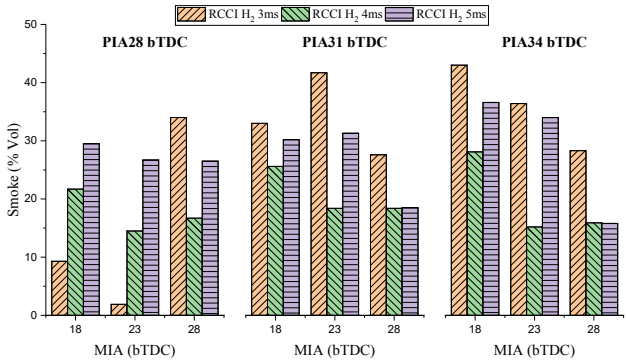


Figure 9. Smoke opacity emissions for split injection WCOBD20-H_2 RCCI.

more combustion efficiency with a reactive controlled approach. Further, too advanced injection timing like PIA31^{0}bTDC and PIA34^{0}bTDC with MIA 18^{0}bTDC also reduces NO_x emissions significantly. This may be due to low reactive fuel with advanced PIA timing creates a homogenous mixture and simultaneous combustion. However, with further increases in hydrogen flow rate and advanced injection timing create improper control of low reactive fuel is created, and excessive reactivity stratification results in too-lean and too-rich zones, resulting in uncontrolled combustion and a sudden rise in cylinder pressure–temperature (hot spots) and thus more NOx emissions.

3.2.4 Smoke Opacity

Smoke opacity can be seen in Figure 9 below. With advanced injection timing of PIA31^{0}bTDC and 34^{0}bTDC, smoke emissions increase. Also, at a low energy share of H_2 3ms injector open time (5.6 LPM), smoke emissions are higher. High reactive fuel in greater quantity causes more rich fuel pockets and more smoke emissions. Further, more dwell in injection timing 13^0-16^0 CA dwell (PIA31^{0}bTDC -MIA18^{0}bTDC and PIA34^{0}bTDC -MIA18^0 bTDC) causes more smoke emissions due to diversified stratified zones. However, notified results shown by advanced injection timing and increased energy share of RCCI low-reactive fuel caused smoke emissions to reduce. This may be due to pre-mixed and homogeneous fuel composition with high flame speed of a greater share of low reactive fuel, causing low smoke formation as a result of simultaneous and controlled combustion. Also, the energy share of 4ms injection timing with dwell timing of 10^0-5^0 CA (PIA28^{0}bTDC -MIA18^{0}bTDC and PIA28^{0}bTDC –MIA23^{0}bTDC has shown lower smoke emissions. This may be due to controlled combustion as a result of moderate stratified zones.

3.3 Performance Analysis

3.3.1 The Energy Share

The contribution of every fuel to total energy input is computed using energy share, therefore influencing combustion control, efficiency, and emissions in RCCI engines. It maximises fuel ratios to support lower emissions, improved performance, and economy of cost. Energy share of hydrogen fuel (low reactive fuel) in the total energy share by both fuels is used as per the formula. below

$$Energy\ share\left(of\ hydrogen\right)=\frac{Heat\ supplied\ by\ hydrogen}{\left(\begin{matrix}Heat\ supplied\ by\ hydroge+\\Heat\ supplied\ by\ WCOBD20\end{matrix}\right)}\times 100$$

The energy share of LRF high octane gaseous hydrogen fuel in total energy (LRF+HRF) is as shown in Figure 10 below. It can be seen that as the high impedance injector open time duration increases LRF hydrogen gas fuel flow quantity increases. It is observed that for 3ms, 4ms, and 5ms injector open time, hydrogen gas flow increases from 5.6 LPM, 10.2 LPM, and 15.1 LPM, respectively. As seen from the figure below, shows influence of injector open time and injection timing strategy has a significant effect on LRF energy share. It can be seen that LRF's energy share increased from 7% to 27%. All operations are carried out at the same power output of 3.5 kW, constant speed 1500 RPM, and same CR18:1. Further interesting results are shown by 4 ms injector open time at MIA 23^{0}bTDC, the energy share of H_2 increases for all PIA, and it is higher

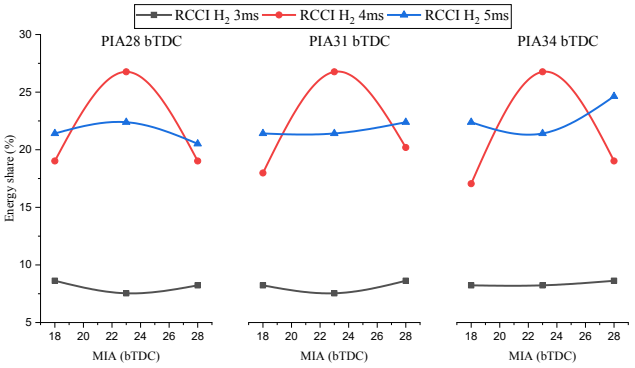


Figure 10. Energy share for split injection WCOBD20-H_2 RCCI.

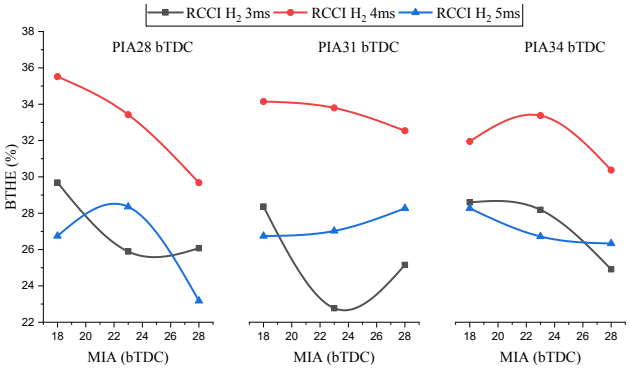


Figure 11. Brake thermal efficiency for split injection WCOBD20-H_2 RCCI.

compared to other MIA timings. This may be due to more reactivity-controlled combustion being achieved as the HRF quantity will be least at this injection timing and LRF operation. This fuel injection timing and RCCI combustion approaches more efficient and controlled combustion. Injector open time with 4ms and injection strategy MIA23^{0}bTDC showed 22% higher energy share compared to 5ms and 74% higher energy share compared to 3ms at the same injection timing. Pilot injection timing has less effect on energy share however MIA has more effect on energy share too retarded MIA18^{0}bTDC and advanced 28^{0}bTDC has report less energy share compared to MIA23^{0}bTDC.

3.3.2 Brake Thermal Efficiency

This influences injection strategy, and RCCI fuel energy share can be seen from Figure 11 below. It can be noted that brake thermal efficiency has an effect of both RCCI, LRF and HRF fuel. Brake thermal efficiency increased from 26.5% to 35% at MIA18^{0}bTDC with the increase in LRF fuel quantity. However, maximum brake thermal efficiency is observed at 4ms injection open time (10.2 LPM), hydrogen flow rate and MIA18^{0}bTDC followed by MIA 23^{0}bTDC with the same PIA28^{0}bTDC. This may be due to more reactivity-controlled combustion, hydrogen energy share (27%), and higher calorific value of hydrogen. However, with hydrogen open time of 5ms with a more hydrogen flow rate (15.1 LPM) has been shown that high flame speed leads to high rich (hot spot) in combustion, rapid HRR, and RPR, causing loss in performance. Further, the advance in MIA from 18 to 28^{0}bTDC has decreased BTHE due to more HRF being burned.

3.3.3 Brake-Specific Fuel Consumption

Brake-specific fuel consumption influences energy share, and the injection strategy can be seen in Figure 12. It can be noted that similar to brake thermal efficiency, energy share of 7%, or 3ms injector open time (5.6 LPM), hydrogen flow rate showed more brake specific fuel consumption. As stated above, BSFC is a measure for both LRF and HRF together at full power operation (100% brake power, 3.5 kW) for all injection timing and LRF operations. Higher brake-specific fuel consumption is followed by 5 ms injection open time (20-21% energy share of hydrogen. Notably least BSFC (0.21 kg/kWhr) is reported by the highest energy share of 27% of hydrogen at MIA23^{0}bTDC and 4 ms injector open time. It can be noted that BSFC slightly increases with an increase in injection advancing both MIA and PIA on the other hand BSFC decreases with retarded injection strategy.

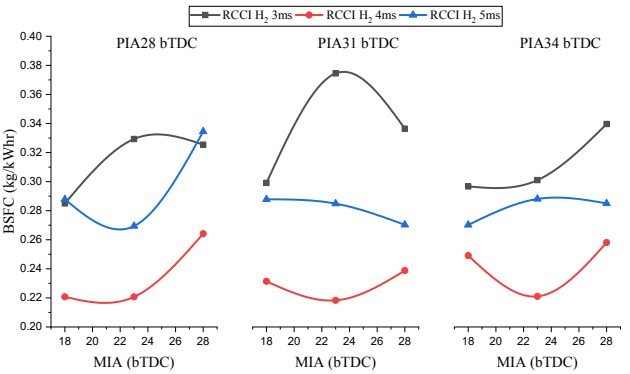


Figure 12. Brake specific fuel consumption for split injection WCOBD20-H_2 RCCI.

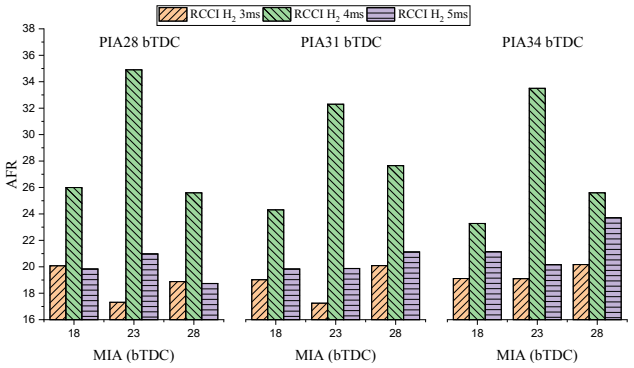


Figure 13. Air fuel ratio for split injection WCOBD20-H_2 RCCI.

3.3.4 Air Fuel Ratio (AFR)

AFR for hydrogen and WCOBD20 total fuel consumed is shown in Figure 13. For LRF hydrogen fuel stoichiometric air-fuel ratio is 27:1, while for HRF, it is 14.6:1. It can be seen from the figure below that the AFR with 4ms injector open time (15.2 LPM) and LRF 27% energy share showed maximum AFR among LRF operations. Also, MIA23^{0}bTDC has reported more AFR. This may be due to homogeneous mixing of hydrogen and air at the inlet, simultaneous reactivity, controlled, more efficient combustion uses less HRF and results in more complete combustion as a consequence of more AFR present. Further moderate AFR is followed by a 5ms injection open time, and less AFR is reported by a 3ms injection open time. This lower AFR by 3ms is due to more HRF fuel being burnt, causing more temperature and less volumetric efficiency.

4.0 Conclusions

1. RCCI combustion with MIA 28^0 bTDC and PIA28^0 bTDC for all H_2 flow rates has shown more combustion pressure among other MIA-PIA operations. It is followed by MIA23^0 bTDC – PIA28^0 and PIA31^0 bTDC. In-cylinder pressure, 50 bar reported by MIA-PIA 28^{0}bTDC 5ms, is the highest among all other operations. The RPR showed that decrease in RPR values with an increase in PIA angle. Further MIA23^0 bTDC-PIA31^{0}bTDC showed RPR up to 3 bar/deg CA. Also, H_2 flow rate with 5ms showed higher RPR for all operations due to more flame speed of hydrogen increasing more rapid combustion.
2. Combustion duration varies from 7ms to 9ms or 65^0 CA to 90^0 CA. It can be seen that at early injection, PIA34^0 bTDC-MIA28^0 bTDC more prolonged combustion duration (prolonged) is observed, leading to knocking and initial high NHR. Also, peak combustion will be before TDC, causing a loss in torque and performance. On the other hand, PIA31^0 and MIA 18^0 and MIA23^0 showed short combustion duration. This leads to a sudden rise in RPR, NHR, and combustion pressure at TDC. This causes uncontrolled combustion. However, PIA28^0 with all RCCI hydrogen energy shared moderate combustion duration and showed a controlled combustion approach. This results in more combustion efficiency, and simultaneous combustion instead of instantaneous combustion in the other two (PIA34^{0}bTDC and PIA31 ^{0}bTDC) injection strategies.
3. LRF causing enriched hydrogen charge into the combustion chamber with early injection of (PIA34^{0}bTDCamd PIA31 ^{0}bTDC with MIA28 ^{0}bTDC) high reactive fuel(HRF) WCOBD20 causes rapid combustion, thus peak raises in HRR are observed. This produces knocking and reduces combustion efficiency similar to retarded injection of MIA18^{0}bTDC and PIA28^{0}bTDC. On the other hand, controlled combustion and NHR are observed at MIA 28^{0}bTDC and PIA28^{0}bTDC as a consequence of not too low NHR or too high NHR.
4. At MIA 23^{0}bTDC and PIA 28^{0}bTDC, HC emissions are reported as are least compared to all other operations. Also, a higher hydrogen flow rate with advanced injection timing of PIA31^0 bTDC and PIA34^0 showed more stratified reach and lean zones, causing more instantaneous combustion. It can be noted that PIA34^0 bTDC and PIA34^0 bTDC show more CO emissions than MIA23^0 bTDC injection timing and 4ms H_2 due to more stratified zones.
5. Nitric oxides emissions with RCCI fuel combination and fuel injection strategy show reduced NOx emissions at MIA23^0 bTDC-PIA28^0 bTDC and 4ms (10.22 LPM) hydrogen fuel flow rate. This may be due to more controlled and reactivity control combustion with a strategic injection timing approach. This injection timing MIA23^0 bTDC-PIA28^0 bTDC, and 4ms (10.22 LPM) hydrogen fuel flow is 50% less compared to the same injection timing and higher hydrogen or WCOBD energy share.
6. Energy share of 27% at 4 ms injection timing with dwell timing of 10^0 -5^0 CA (PIA28^{0}bTDC -MIA18^{0}bTDC and PIA28^{0}bTDC –MIA23^{0}bTDC have shown lower smoke emissions. This may be due to controlled

combustion as a result of moderate stratified zones. Smoke opacity showed that with advanced injection timing of PIA31^{0}bTDC and 34 ^{0}bTDC, smoke emissions increase. Also, at a low energy share of H_2 3ms injector open time (5.6 LPM), smoke emissions are higher. Further, more dwell in injection timing 13^0 -16^0 CA dwell (PIA31^{0}bTDC -MIA18^{0}bTDC and PIA34^{0}bTDC -MIA18^0 bTDC) causes more smoke emissions due to diversified stratified zones.

7. Energy share for injector open time 4ms and MIA23^0 bTDC-PIA28^0 bTDC has noted the highest energy share compared to 5 ms injector open time and 3 ms injector open time, and other MIA-PIA. Brake thermal efficiency increased from 26.5% to 35% at MIA18^{0}bTDC with an increase in LRF fuel quantity. However, maximum brake thermal efficiency is observed at 4 ms injection open time (10.2 LPM), hydrogen flow rate and MIA18^{0}bTDC followed by MIA 23^{0}bTDC with the same PIA28^{0}bTDC. This may be due to more reactivity-controlled combustion, hydrogen energy share (27%), and higher calorific value of hydrogen.
8. It can be noted that similar to brake thermal efficiency, energy share of 7%, or 3ms injector open time (5.6 LPM), hydrogen flow rate showed more brake specific fuel consumption, followed by 5 ms injection open time (20-21% energy share of hydrogen. Notably least BSFC (0.21 kg/kWhr) is reported by the highest energy share of 27% of hydrogen at MIA23^{0}bTDC and 4 ms injector open time. Also, for the same operation maximum of AFR 34 is reported due to reactivity-controlled and homogenous combustion.

5.0 References

1. Yaopeng L, Ming J, Yaodong L, Maozhao X. Numerical study on the combustion and emission characteristics of a methanol/diesel reactivity controlled compression ignition (RCCI) engine. Appl Energy. 2013; 106:184-197. https://doi.org/10.1016/j.apenergy.2013.01.058
2. Splitter DA, Reitz RD. Fuel reactivity effects on the efficiency and operational window of dual fuel compression ignition engines. Fuel. 2014; 118:163-175. https://doi.org/10.1016/j.fuel.2013.10.045
3. Benajes J, Molina S, Garcia A, Belarte E, Vanvolsem M. An investigation on RCCI combustion in a heavy-duty diesel engine using in-cylinder blending of diesel and gasoline fuels. Appl Therm Eng. 2014; 63:66-76. https://doi.org/10.1016/j.applthermaleng.2013.10.052
4. Li J, Yang WM, Goh TN, An H, Maghbouli A. Study on RCCI (reactivity controlled compression ignition) engine by means of statistical experimental design. Energy. 2014; 78:777-787. https://doi.org/10.1016/j.energy.2014.10.071
5. Desantes JM, Benajes J, Garcia A, Serrano JM. The role of the in-cylinder gas temperature and oxygen concentration over low load reactivity controlled compression ignition combustion efficiency. Energy. 2014; 78:854-868. https://doi.org/10.1016/j.energy.2014.10.080
6. Yaopeng L, Ming J, Yachao C, Yaodong L, Maozhao X, Tianyou W. Parametric study and optimization of a RCCI (reactivity controlled compression ignition) engine fueled with methanol and diesel. Energy. 2014; 65:319-332. https://doi.org/10.1016/j.energy.2013.11.059
7. Paykani A, Kakaee AH, Rahnama P, Reitz RD. Effects of diesel injection strategy on natural gas/diesel reactivity controlled compression engine combustion. Energy. 2015; 90:814-826. https://doi.org/10.1016/j.energy.2015.07.112
8. Reitz RD. Directions in internal combustion engine research. Combust Flame. 2013; 160(1):1-8. https://doi.org/10.1016/j.combustflame.2012.11.002
9. Kakaee AH, Rahnama P, Paykani A. Influence of fuel composition on combustion and emissions characteristics of natural gas/diesel RCCI engine. J Nat Gas Sci Eng. 2015; 25:58-65. https://doi.org/10.1016/j.jngse.2015.04.020
10. Charitha V, Thirumalini S, Prasad M, Srihari S. Investigation on performance and emissions of RCCI dual fuel combustion on diesel-biodiesel in a light-duty engine. Renew Energy. 2018; Available from: https://doi.org/10.1016/j.renene.2018.09.048 https://doi.org/10.1016/j.renene.2018.09.048
11. Jing L, Wenming Y, Dezhi Z. Review on the management of RCCI engines. Renew Sustain Energy Rev. 2017; 69:65-79. https://doi.org/10.1016/j.rser.2016.11.159
12. Ansari E, Shahbakhti M, Naber J. Optimization of performance and operational cost for a dual-mode diesel-natural gas RCCI and diesel combustion engine. Appl Energy. 2018; 231:549-561. https://doi.org/10.1016/j.apenergy.2018.09.040
13. Zheng Z, Xia M, Liu H, Shang R, Ma G, Yao M. Experimental study on combustion and emissions of n-butanol/biodiesel under both blended fuel mode and dual fuel RCCI mode. Fuel. 2018; 226:240-251. https://doi.org/10.1016/j.fuel.2018.03.151
14. Deheri C, Acharya SK, Thatoi DN, Mohanty AP. A review on performance of biogas and hydrogen on diesel engine in dual fuel mode. Fuel. 2020; 260:116337. https://doi.org/10.1016/j.fuel.2019.116337

15. Khan TMY, Soudagar MEM, Khandal SV, Javed S, Mokashi I, Baig MAA, *et al*. Performance of Common Rail Direct injection (CRDi) engine using *Ceiba Pentandra* biodiesel and hydrogen fuel combination. Energies. 2021; 14(21):1-16. https://doi.org/10.3390/en14217142
16. Shaikh SM, Khandal SV. Studies on biodiesel and hydrogen-powered dual fuel common rail direct injection engine. Indian J Sci Technol. 2024; 17(10):917-923. https://doi.org/10.17485/IJST/v17i10.3194
17. Wategave SP, Banapurmath NR/ Combustion and emission characteristics of RCCI engine fueled with hydrogen and karanja biodiesel renewable fuels. International Journal of Hydrogen Energy. 2025; 123,:184-193. https://doi.org/10.1016/j.ijhydene.2025.03.409
18. TV1 Engine Parameters : Make - Kirloskar oil, Model -TV1, Type-Single cylinder, 4 stroke diesel, water cooled,power 5.2 kw at 1500 rpm, stroke 110, compression ratio 17.5, capacity 661 cc, IS-11170 Code 18.1324 Available from: https://drive.google.com/file/d/0BxpHpyYTEWVdMUFjWkxyc0c0VUk/view?resourcekey=0-nVvZ9wWTCzO93O7CmpD6hQ